ELSEVIER

Colloids and Surfaces
A: Physicochemical and Engineering Aspects 190 (2001) 89–98

COLLOIDS AND SURFACES A

www.elsevier.com/locate/colsurfa

Microstructure and rheological behaviour of electrosterically stabilized silica particle suspensions

Jae-Hyun So [2], Seung-Man Yang [2,*], Chongyoup Kim [1], Jae Chun Hyun [1]

[1] *Department of Chemical Engineering and Applied Rheology Center, S-1 Anam-dong, Sungbuk-gu, Seoul 136-701, South Korea*
[2] *Department of Chemical Engineering, Korea Advanced Institute of Science and Technology, 373-1 Kusong-dong, Yusong-gu, Taejon 305-701, South Korea*

Abstract

In the present study, microstructural transitions of silica suspensions were examined by rheological measurements under either steady simple shear or oscillatory flow. First, monodisperse silica particles were prepared by the so-called modified Stöber method and were stabilized sterically in organic medium. Silane coupling agent, such as 3-(trimethoxysilyl)propyl methacrylate or *N*-[3-(trimethoxysilyl)propyl] ethylenediamine (aminosilane coupling agent) was coated onto the particle surface to induce steric stabilization at various volume fractions (ϕ) up to $\phi = 0.45$. To ensure 'hard' sphere suspension, the silica particles were dispersed in a refractive-index matching solvent, tetrahydrofurfuryl alcohol, in which the van der Waals dispersion forces diminished. Second, charge stabilized silica particles were prepared in aqueous medium. In this case, ionic strength was adjusted by KCl concentration after surface modification with amino silane coupling agent. The charge stabilized suspension showed stable shear-thinning behaviour, which was well contrasted by the hard sphere suspension. The latter exhibited negligible electrostatic repulsion and only short-range interactions. Finally, microstructural transition of aqueous silica suspensions from liquid- to solid-like structure was examined in terms of particle volume fraction and salt concentration. © 2001 Elsevier Science B.V. All rights reserved.

Keywords: Silica suspension; Microstructural transition; Charge stabilization; Soft and hard spheres; Rheological behaviour

1. Introduction

The flow behaviour and microstructure of particle dispersions have been studied intensively because of their practical significance in paints, polymers, ceramics, composite materials, electronic industry, coating process and so on. In particular, metal oxide suspensions have attracted considerable attention in the electronic industry [1,2]. Generally, particle dispersion shows highly non-Newtonian behaviour even though the medium is a Newtonian liquid. Deviation from the Newtonian flow behaviour becomes pronounced at high particle volume fractions and under strong flow field. As the imposed flow becomes strong, semi-dilute and concentrated suspensions often exhibit shear thickening, following a gradual decrease in the shear viscosity. Practically, continuous or discontinuous shear thicken-

* Corresponding author.
E-mail address: smyang@kaist.ac.kr (S.-M. Yang).

0927-7757/01/$ - see front matter © 2001 Elsevier Science B.V. All rights reserved.
PII: S0927-7757(01)00668-9

ing causes severe damages on the particulate process and eventually deteriorates productivity [3,4]. Therefore, it is necessary to investigate the microstructural changes of particulate suspensions, and thereby to control the rheological properties under flow field. The flow characteristics of particulate suspensions can be controlled by the particle shape and size distribution, interparticle forces, and the volume fraction of the dispersed phase [1–4].

In general, monodisperse hard sphere suspension begins to order into a macrocrystalline structure of face centred cubic or hexagonally close packing, when the particle volume fraction (ϕ) exceeds 0.5 under equilibrium condition with no imposed flow. Further, when $0.5 < \phi < 0.55$, the random disordered phase and the colloidal crystalline phase coexist [5–7]. However, charge stabilized suspensions form macrocrystalline structure at much below volume fractions compared to hard sphere suspensions. This is because particles in an electrostatically stabilized suspension experience much stronger long-range repulsive interactions than hard spheres [5,8–11]. Charge stabilized polymer latices such as polystyrene or polymethalmethacrylate show 'soft' sphere behaviour and rheological responses of these latex suspensions have been studied extensively [10–12]. Recently, some works have been reported for silica or alumina particle suspension [13,14].

In the present study, the rheological behaviour was examined for semi-dilute charge stabilized silica suspensions by varying the strength of interparticle forces. Monodisperse silica particles have been synthesized successfully through sol–gel method [15–24]. In particular, Jansen et al. [16] prepared amorphous silica particles according to Stöber's method and esterified the surface silanol groups of the electrostatically stabilized particle with octadecyl alcohol, which rendered the particle lyophilic and readily dispersible in nonpolar (organic) solvents. More recently, the stabilization effects and microstructural changes for hard sphere silica suspensions have been considered in our group by using various silane coupling agents, vinyltriethoxy silane, γ-methacryloxypropyl triethoxy silane and 3-(trimethoxysilyl)propyl methacrylate (MPTS) [20,22,24]. Through the sol–gel method via hydrolysis and condensation of silicon alkoxide, tetraethylorthosilicate (TEOS), monodisperse silica particles were synthesized for the dispersed phase. The monodisperse silica particles were stabilized with a silane coupling agent and used for the preparation of sterically stabilized suspension in either organic or aqueous medium. In general, silica particles in aqueous medium possess surface charge, and thus the silica particles are stabilized predominantly by electrostatic repulsion since the thickness of steric barrier is much smaller than the range of the electrostatic repulsion. The electrostatic repulsion can be controlled by varying ionic strength (or salt concentration) and pH. In the subsequent sections, the rheological responses of the silica suspensions were examined as functions of the particle size and volume fraction. In addition, we examined the microstructural transition of aqueous silica suspensions from liquid- to solid-like structure by monitoring the storage (G') and loss (G'') moduli for various particle volume fractions and salt concentrations.

2. Experimental

Monodisperse silica particles were synthesized through the sol–gel method in ethanol medium (Oriental) proposed by Stöber et al. [15]. TEOS ($Si(OC_2H_5)_4$; Aldrich) and deionized water were used as reactants for preparation of the spherical silica particles with the aid of reaction catalyst, ammonium hydroxide (Aldrich). The ethanol was used after distilled twice and all other chemicals were used as received. The particle size was controlled by varying water and ammonia contents. In order to prepare concentrated and mono-disperse silica suspensions, hydrolysis and condensation reactions were carried step-wisely with time interval of 12 h as suggested by Bogush et al. [17]. Detailed reactant compositions, particle sizes and surface areas prepared by a single step and three step synthetic processes were compared in Table 1.

To enhance the phase stability of electrically neutral silica suspensions, MPTS ($(CH_3O)_3Si$-$(CH_2)_3OCOC(CH_3)=CH_2$; Aldrich) were coated on the silica particles by chemical adsorption after step-wise particle synthesis and subsequent purification, which was conducted by a few times of washing and ultracentrifugation. To ensure hard sphere suspensions by screening the van der Waals attraction, tetrahydrofurfuryl alcohol (THFFA; Aldrich) was used as a refractive-index matching solvent ($n_D = 1.45$). Through the surface modification of silica particles, any residual interparticle interaction could be removed effectively and showed nearly 'hard sphere' behaviour. Detailed procedure of the surface modification and adsorption behaviour of MPTS onto silica particles were described in our previous reports [22,24]. Meanwhile, charged stabilized silica suspensions, which have long-range repulsive interactions, were prepared in aqueous medium after surface modification with amino silane coupling agent, *N*-[3-(trimethoxysilyl)propyl] ethylenediamine ($(CH_3O)_3Si(CH_2)_3NHCH_2CH_2NH_2$)). Synthesized stock silica particles were washed with deionized water and ultracentrifuged five or six times in order to remove residual reactants and purify silica particle surface. Then, the cleaned silica particles dispersed in deionized water were coated with excess amount of 10^{-1} M amino silane coupling agent, *N*-[3-(trimethoxysilyl)propyl] ethylenediamine. After the surface modification with amino silane coupling agent for 12 h, silica particles were separated from the mixture by ultracentrifugation and re-dispersed in distilled water, of which the ionic strength was controlled by changing KCl concentration from 10^{-3} to 10^{-1}M. In order to increase the particle loading, the silica suspension was dialyzed against dilute aqueous polyethyleneglycol (molecular weight: 20 000; Junsei) solution. During dialysis, the salt concentration was adjusted by using dialysis membrane of which the molecular weight cut-off is in the range of 6000–8000. The KCl dialysis solutions with dissolved PEG were replaced with fresh one several times in 48 h and then the particle suspensions were aged for at least 1 week. The concentrated suspensions with low salt concentration were slightly iridescent or had a slightly bluish hue because of Bragg diffraction.

The density of silica particle is necessary to determine the particle volume fraction in the suspension. In this work, the density of the suspended silica particle was estimated from the intrinsic viscosity of monodisperse spherical suspension at extreme dilutions. By measuring the viscosity for extremely dilute suspensions using an Ubbelohde capillary viscometer, the density of prepared silica particles was determined from the fact that the intrinsic viscosity must be 5/2 [20,22,24]. Small amount of the suspension, usually 1 g, was placed in glass vials and dried to constant mass at 110°C. The weight fraction of each suspension was converted to the volume fraction using the pre-determined density of each silica particle.

For charged silica particles, ζ-potential of silica suspension was measured by electrophoretic light scattering (Brookhaven) and the result is shown in Table 2. The rheological behaviour was monitored by an Advanced Rheometric Expansion

Table 1
Compositions of the reactants in a single step and three step growth reactions, mean radius and BET surface area of the model silica particles

Sample	Seed composition (M)	1st TEOS (M)	2nd TEOS (M)	3rd TEOS (M)	Mean radius (nm)	BET surface area ($m^2\ g^{-1}$)
S13	$[TEOS] = 0.57$, $[NH_3] = 0.35$, $[H_2O] = 0.85$	0.57	0.57	0.57	l08.52 ± 5.55	13.04
S51	$[TEOS] = 0.57$, $[NH_3] = 0.71$, $[H_2O] = 5.0$	0.57	–	–	272.78 ± 1.97	5.966

Table 2
pH and ζ-potential of the silica particle suspensions

Sample	Bare silica suspension [KCl] = 10^{-3} M	Surface modification with amino silane in aqueous solvent			Surface modification with MPTS in THFFA
		[KCl] = 10^{-3} M	[KCl] = 10^{-2} M	[KCl] = 10^{-1} M	
S13	-52.7 ± 2.5 mV (pH = 9.13)	-48.6 ± 2 8 mV (pH = 8.86)	-39.4 ± 2.1 mV (pH = 8.48)	-12.8 ± 4.5 mV (pH = 8.45)	-0.9 ± 0.4 mV
S“51	-63.3 ± 2.9 mV (pH = 8.88)	-47.2 ± 3.8 mV (pH = 8.10)	–	–	-0.8 ± 0.5 mV

System under either steady or oscillatory shear flow in Couette geometry. The series of steady shear viscosity measurements were performed after samples were pre-sheared at a constant shear rate of 0.025 s^{-1} for 60 s. Frequency sweep measurements in oscillatory shear flow were carried in the range of linear viscoelasticity determined by strain sweep test. All rheological measurements were conducted at a fixed temperature of 25°C.

3. Results and discussions

3.1. Characterization of the stabilized silica suspensions

The synthesized monodisperse silica particles were spherical and the average particle radii of S13 and S51 were 108.52 ± 5.52 and 272.78 ± 1.97 nm, respectively. TEM images of these silica particles were reproduced in Fig. 1. It can be noted that high ammonia content produced large particles with uniform size distribution. In order to prepare the silica suspensions at various particle loadings, it is needed to determine the density of the suspended silica particle. Spherical particle density can be determined from the intrinsic viscosity of the suspension at extreme dilutions. We measured the shear viscosity of extremely dilute suspensions using an Ubbelohde capillary viscometer and the relative viscosity was plotted as a function of the particle volume fraction for smaller and larger particle suspensions. According to Einstein's theory, the intrinsic viscosity should be 5/2 for a spherical particle suspension. By fitting the viscosity data at extremely dilute concentrations to Einstein's theory, the densities of the prepared silica particles were determined as 1.62×10^{-3} and 1.70×10^{-3} kg m^{-3} for S13 and S51, respectively. These values of the particle density were very close to the previous results [18,22,24–26]. Finally, the silica suspensions at various volume fractions could be prepared in aqueous media or THFFA solvent using the measured density of each silica particle.

Surface properties and steady shear viscosities of 'hard sphere' silica suspension in a refractive-index matching solvent THFFA after MPTS coating (denoted as HS13 and HS51) were characterized in our previous report [24]. Adsorption behaviour of MPTS onto silica particles were analyzed by UV–visible spectroscopy, and the result fitted to Langmuir-type adsorption equation was shown in Fig. 2(a). In addition, as noted from Table 2, the silica particles in aqueous medium possess substantial surface charges, and in charge-stabilized suspensions, they exhibit 'soft sphere' characteristics i.e., long-range repulsive forces exist. Although the silica particles were stabilized by electrostatic repulsion induced by electrical double layer, surface modification was conducted with amino silane coupling agent to give additional steric repulsion. By the surface modification of silica surface with silane coupling agent, possible flocculation of silica particles could be prevented at high ionic strengths. However, when the salt concentration [KCl] is as low as 10^{-3} M, the thickness of double layer formed on the silica particle is extended to a larger distance than the steric barrier of aminosilane. Thus,

at low salt contents, silica particles were predominantly stabilized by electrostatic repulsion forces.

To confirm the adsorption of amino silane coupling agent onto the silica particles, the adsorbed amount of amino silane coupling agent was measured by monitoring the nitrogen element through element analysis. The amino silane coupling agent forms steric barrier and leads to the particle stability in aqueous medium. This is owing to the reaction of surface silanol group of silica and methoxy group of silane coupling agent. After surface modification with amino silane coupling agent, silica particles were separated from the mixture of amino silane coupling agent and aqueous stock silica suspension by ultracentrifugation. The adsorbed amounts of nitrogen were determined using element analysis and normalized with the results for bare silica particles. The results were reproduced in Fig. 2(b), in which the adsorption isotherms were fitted with Langmuir-type adsorption equation. It can be seen from those adsorption isotherms that the effect of ammonium hydroxide catalyst was considerable in the adsorption of silane coupling agent. Although the normalized adsorbed amounts for different sized particles is usually fitted on the same curve, the chemically adsorbed amounts of silane coupling agent deviate due to the strong effect of ammonium hydroxide used in the synthesis step. However, it should be noted that the adsorbed amount of silane coupling agent onto the silica particles was small compared to its bulk concentration. Therefore, the particle purification was very important step and the surface modified silica particles must be purified more than five times by successively adding high purity solvent and removing the supernatant after each ultracentrifugation.

The appreciable size change was not observed by TEM after silane coupling agent adsorption onto the silica surface, implying that the coated layer should be negligibly thin compared with the primary particle size [20,22,24]. In addition, we measured ζ-potential through the electrophoretic mobility of the bare and surface modified silica particles using electrophoretic light scattering system. The ζ-potential of each silica suspension was shown in Table 2 for various salt concentrations in either aqueous or organic medium. As noted, for both bare and salt controlled suspensions, pH was around 8–9. Thus, for aqueous suspensions, pH was maintained far above the isoelectric point although it slightly decreased by surface modification and salt addition. In case of the MPTS coated silica particle in organic solvent, the ζ-potential was very small and nearly negligible. Meanwhile, the silica particles that were coated with aminosilane and dispersed in aqueous media showed slightly weaker ζ-potential than bare silica particles. This is due mainly to the surface terminated amino groups. However, the coated silica particles still possessed highly negative ζ-po-

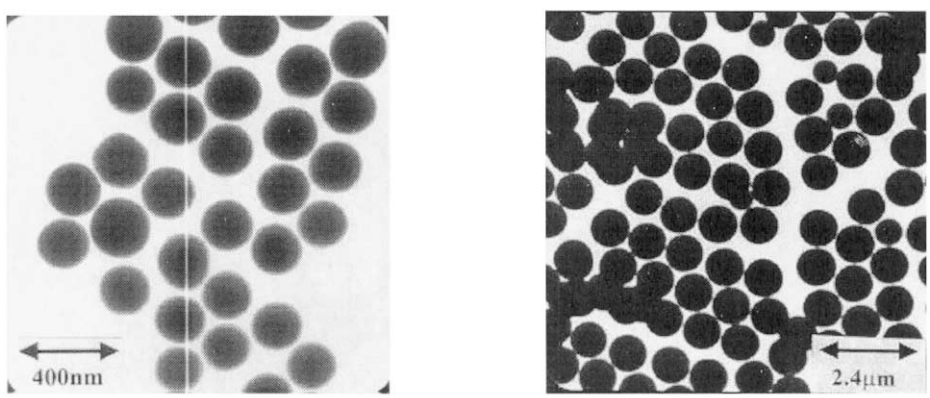

Fig. 1. TEM images of the prepared silica particles: (a) for particles S13, and (b) for particles S51.

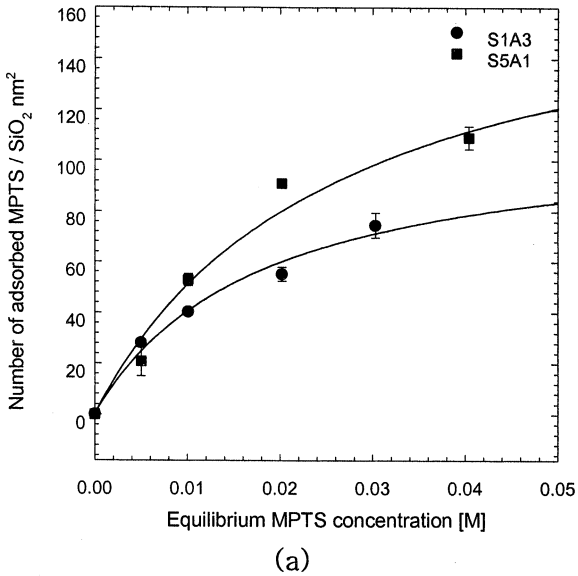

Fig. 2. Adsorption isotherms of silane coupling agent onto the silica particles: (a) MPTS, and (b) amino silane coupling agent.

tential and were effectively stabilized by surface charge. Moreover, the density of surface charge was decreased as KCl concentration increased. This clearly indicates that addition of salts decreases both the range and the magnitude of electrostatic repulsion by reducing the Debye shielding length and the ζ-potential [14].

3.2. Rheological behaviour and microstructure transitions of silica suspensions

Significant deviations from Newtonian behaviour were induced by the combined contributions from the hydrodynamic and non-hydrodynamic interparticle interactions and random Brownian motions under a uniform shear field. It can be simply expected that increment in the particle content decreases the interparticle distance, and consequently leads to considerable changes in the flow properties of the suspension. Thus, rheological behaviour of the semi-dilute or concentrated suspensions may be very complicated compared to other homogeneous fluids. In Fig. 4, shear viscosity of S13 suspension was plotted as a function of the shear rate for three different volume fractions of $\phi = 0.371$, 0.400 and 0.427. In this plot, the salt concentration was adjusted to 10^{-3} M. The shear viscosity of the S13 particle suspensions, of which the salt concentration was adjusted to 10^{-2} M was also included in Fig. 4. Typical shear thinning behaviour was observed for semi-dilute charge stabilized suspension of S13 for both the salt concentration of 10^{-3} and 10^{-2} M. It can be noted from comparison of Figs. 3 and 4 that as the salt concentration increased, the shear viscosity was reduced. This can be explained by the fact that the screening effect of added salt, and consequent compression of electrical double layer lead to the decrease of effective volume fraction. Indeed, as noted from Table 2, the magnitude of ζ-potential was decreased with the increase in ionic strength. Moreover, the decrease in shear viscosity was much pronounced at low shear rates where interparticle force was dominant. It can be also seen that when the particle volume fraction was lower than 0.400, the zero-shear-rate viscosity was measurable. This is because, at low particle volume fractions, the suspension was nearly random and isotropic structure and behaved like Newtonian fluids. Therefore, the viscosity at low shear rates showed a Newtonian plateau. Meanwhile, when the particle loading exceeded 0.400, the suspensions did

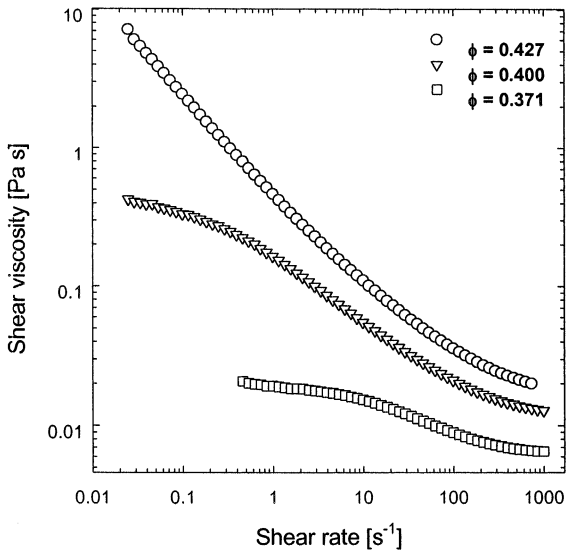

Fig. 3. Shear viscosity as a function of the shear rate for S13 with [KCl] = 10^{-3} M.

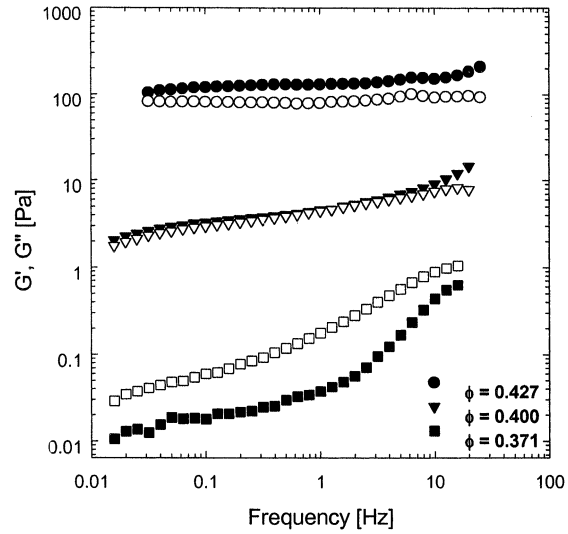

Fig. 5. Storage (G'; filled symbol) and loss (G''; open symbol) moduli as a function of the frequency for S13 suspensions with [KCl] = 10^{-3} M.

not exhibit the zero-shear-rate viscosity, and instead the viscosity shear thinned continuously. This is due to the fact that some microstructure was formed at high concentrations at equilibrium, and this microstructure was deformed under the imposed shear flow. The effects of salt concentration on the rheological properties shall be discussed shortly.

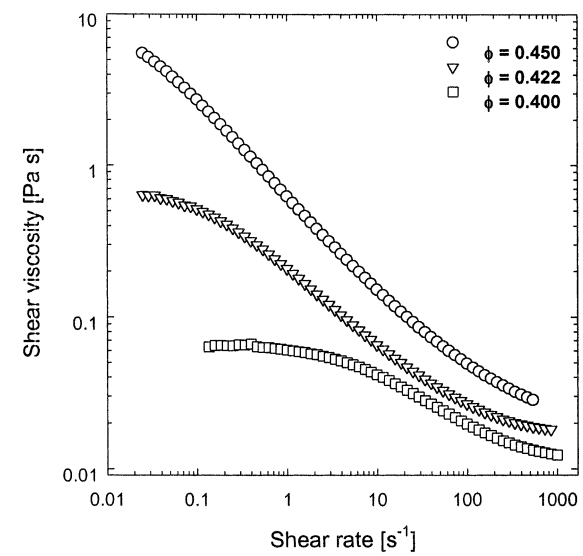

Fig. 4. Shear viscosity as a function of the shear rate for S13 with [KCl] = 10^{-2} M.

In order to examine the microstructure of S13 suspension with the salt concentration fixed at 10^{-3} M, storage (G') and loss (G'') moduli were measured as a function of the sweep frequency and the result is reproduced in Fig. 5. Although both the storage and loss moduli increased with the volume fraction, the increase in G' was steeper than that of G''. Therefore, at low volume fractions ($\phi \leqslant 0.400$), the loss modulus G'' was larger than or equal to the storage modulus G'. Also noted is that both the storage and loss moduli at low volume fractions ($\phi \leqslant 0.400$) increased monotonously with the frequency. This is clearly indicative of the fact that the suspension at low volume fractions exhibited typical liquid-like behaviour. However, as the volume fraction exceeded 0.400, G' and G'' were nearly independent of the frequency. In addition, the storage modulus G' was larger than the loss modulus G'' at $\phi \geqslant 0.400$. The behaviour of G' and G'' as a function of the particle volume fraction and frequency clearly indicates that the microstructure of S13 suspension changes from liquid- to solid-like structure as the volume fraction increases. Furthermore, the overall feature of dynamic response

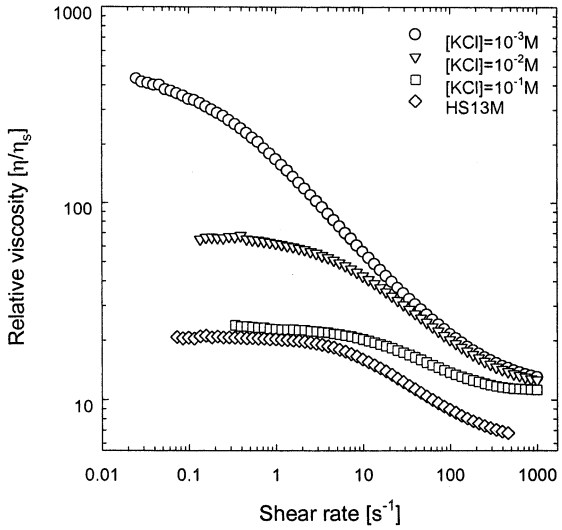

Fig. 6. Relative viscosity as a function of the shear rate for S13 at $\phi = 0.400$.

(G' and G'') was consistent with the previous shear viscosity behaviour.

In Figs. 6 and 7, the effects of the ionic strength on shear viscosity, storage and loss moduli were illustrated for the volume fraction fixed at $\phi = 0.400$. First, the relative viscosity (i.e., suspension viscosity scaled by pure solvent viscosity) of

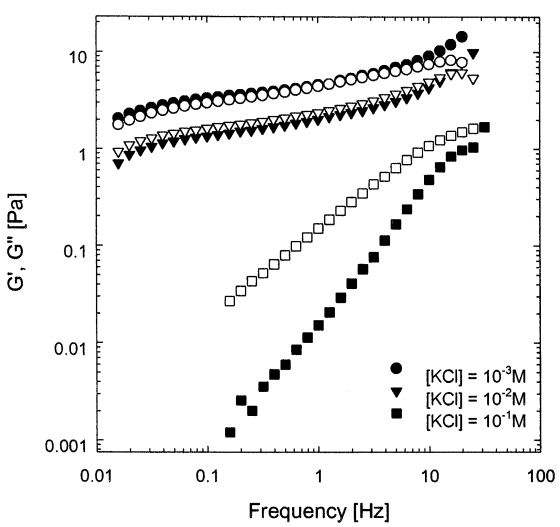

Fig. 7. Storage (G'; filled symbol) and loss (G''; open symbol) moduli as a function of the frequency for S13 suspensions at $\phi = 0.400$.

charge stabilized suspensions at $\phi = 0.400$ was given in Fig. 6 for various salt concentrations. Also included in Fig. 6 for comparison is the relative viscosity of the 'hard sphere' suspension of HS13. It can be readily noted that as the salt concentration increased, the relative viscosity decreased and approached the viscosity of the hard sphere suspension. This clearly implies that the long-range repulsive force diminished with ionic strength and charged particles at high salt concentrations behaved like hard spheres. As mentioned earlier, the increase in salt concentration enhances the screening effect and compresses the electric double layer, which reduces the depletion volume and consequently decreases the effective particle volume fraction. In particular, the change in shear viscosity as a function of the salt concentration was pronounced at low shear rates in which the interparticle forces were dominant rather than hydrodynamic forces imposed by the shear flow. As the shear rate increased, the hydrodynamic contribution became dominant and the shear viscosities of charge-stabilized suspensions approached the viscosity of the hard sphere suspension with no interparticle interaction. This is independent of the salt concentration but dependent of the apparent particle volume fraction. In Fig. 7, the storage and loss moduli was plotted as a function of the frequency for the same set of parameters as in Fig. 6. It can be easily seen that the loss modulus is larger than the storage modulus when the salt concentration is above 10^{-2} M. Also noted is that both the moduli decreased with the ionic strength. Indeed, at high salt concentrations, the charge stabilized suspensions displayed liquid-like behaviour at the volume fraction $\phi = 0.400$. However, at a lower salt content, the trend was reversed. At a very low salt concentration $[KCl] = 10^{-3}$ M, the storage (G') and loss (G'') moduli of the S13 suspension with the volume fraction of $\phi = 0.400$ showed very weak dependence on the frequency and G' is slightly larger than G''. Thus, at low salt concentrations, the charge stabilized suspensions exhibited solid-like behaviour, especially at low frequencies.

In order to examine the particle size effect on the rheological behaviour and microstructural

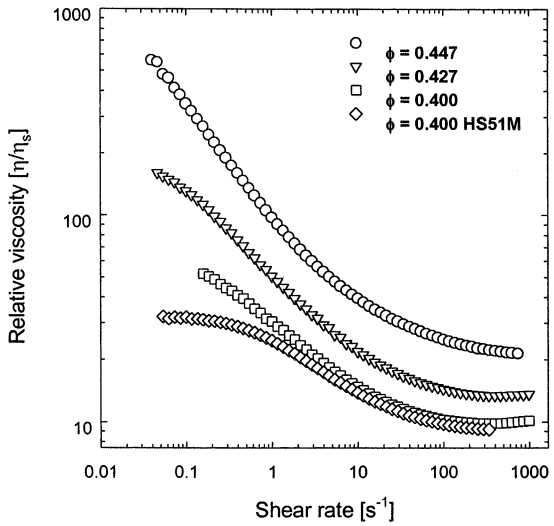

Fig. 8. Relative viscosity as a function of the shear rate for S51 suspensions with $[KCl] = 10^{-3}$ M.

transition, the shear viscosity, storage (G') and loss (G'') moduli of S51 suspension were measured for various particle volume fractions. It is noteworthy at this point that the particle size of S51 was two times larger than that of S13. The relative viscosity was plotted as a function of the shear rate for three different volume fractions of $\phi = 0.447$, 0.427 and 0.400, and the result was reproduced in Fig. 8. Also shown for comparison is the relative viscosity of the hard sphere suspension HS51. The overall features of shear viscosity as shown in Fig. 6 were preserved for the larger particle suspensions. The so-called Stokesian dynamics simulation shows that Brownian contribution to the shear stress diminishes leaving only the hydrodynamic contribution as the shear rate increases [27–30]. The disappearance of the Brownian contribution leads to a viscosity reduction, i.e., shear thinning since the Brownian fluctuations tend to form a random disordered structure. It is also obvious that the Brownian contribution to a suspension of the smaller particles can be sustained at the higher shear rates. In addition, at a given volume fraction, the interparticle interaction becomes stronger for smaller particle suspension due to closer interparticle distance. Thus, for a given particle volume fraction, the suspension of smaller particles S13 possesses the higher viscosity at low shear rates.

The storage (G') and loss (G'') moduli of S51 suspension were measured as a function of the frequency for the salt concentration fixed at 10^{-3} M, and the result was shown in Fig. 9. Similarly to the case of S13 suspension, the loss modulus G' showed higher value than the storage modulus G'' at lower volume fractions ($\phi \leqslant 0.400$), and both the moduli are strongly dependent on the frequency. This is again indicative of liquid-like structure at low particle loadings. However, as the volume fraction increased above $\phi = 0.400$, G' and G'' were nearly independent of the frequency and G' is slightly larger than G''. Thus, the dynamic behaviour of G' and G'' clearly indicates that the transition from liquid- to solid-like structure occurs at about $\phi = 0.400$ for a given salt concentration 10^{-2} M.

4. Summary

In the present paper, the monodisperse silica suspensions were prepared by sol–gel method and

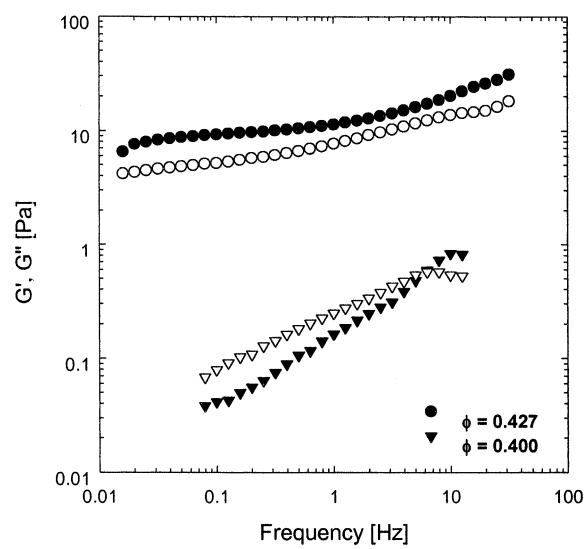

Fig. 9. Storage (G'; filled symbol) and loss (G''; open symbol) moduli as a function of the frequency for S51 with $[KCl] = 10^{-3}$ M.

their rheological behaviour and microstructural transition were investigated experimentally. In particular, the shear viscosity of charge stabilized was measured and compared with the viscosity of hard sphere suspensions that have only short-range interactions. Moreover, the storage (G') and loss (G'') moduli of the silica suspensions were measured to probe the transition from liquid- to solid-like structure by varying the particle volume fraction, salt concentration and particle size. The conclusions from the present investigations are as follows:

(1) The electrostatic repulsive forces of charge-stabilized suspensions were controlled by the salt concentration. As the salt concentration increased, the effective volume fraction of charge-stabilized suspension was decreased, the shear viscosity approached to the viscosity of hard sphere suspension.

(2) For a smaller particle suspension of S13, elastic and solid-like response was enhanced as the particle volume fraction increased. The transition volume fraction was about $\phi = 0.400$ for a given salt concentration of $[KCl] = 10^{-2}$ M. However, as the salt concentration increased, the transition volume fraction was increased.

(3) For a larger particle suspension of S51, similar viscoelastic responses as in a smaller particle suspension S13 were observed. However, the viscosity at low shear rates was decreased as the particle size increased. This is due to the fact that the Brownian motion contribution diminished for the larger particle suspension.

Acknowledgements

This work was supported by a grant from the Ministry of Commerce, Industry and Energy. The authors also acknowledge partial supports from the Brain Korea 21 project and from the Applied Rheology Center.

References

[1] Th.F. Tadros, Adv. Colloid Interface Sci. 68 (1996) 97.
[2] J.-H. So, M.-H. Oh, J.-D. Lee, S.-M. Yang, J. Chem. Eng. Jpn., 2001 34 (2001) 262.
[3] H.A. Barnes, J.F. Hutton, K. Walters, An Introduction to Rheology, Elsevier, New York, 1989.
[4] H.A. Barnes, J. Rheology 33 (1989) 329.
[5] W.B. Russel, D.A. Saville, W.R. Schowalter, Colloidal Dispersion, Cambridge University Press, New York, 1989.
[6] A.P. Gast, W.B. Russel, Phys. Today 51 (12) (1998) 24.
[7] R.G. Larson, The Structure and Rheology of Complex Fluids, Oxford University Press, New York, 1999.
[8] A. Kose, M. Ozaka, K. Takano, Y. Kobayashi, S. Hachisu, J. Colloid Interface Sci. 44 (1973) 330.
[9] A. Kose, S. Hachisu, J. Colloid Interface Sci. 55 (1976) 487.
[10] L.B. Chen, B.J. Ackerson, C.F. Zukoski, J. Rheology 38 (1994) 193.
[11] M.K. Chow, C.F. Zukoski, J. Rheology 39 (1995) 33.
[12] H.M. Laun, R. Bung, S. Hess, W. Loose, O. Hess, K. Hahn, E. Hadicke, R. Hingmann, F. Schmidt, P. Lindner, J. Rheology 36 (1992) 743.
[13] M.E. Fagan, C.F. Zukoski, J. Rheology 41 (1997) 373.
[14] G.V. Franks, Z. Zhou, N.J. Duin, D.V. Boger, J. Rheology 44 (2000) 759.
[15] W. Stöber, A. Fink, E. Bohn, J. Colloid Interface Sci. 26 (1968) 62.
[16] J.W. Jansen, C.G. de Kruif, A. Vrij, J. Colloid Interface Sci. 114 (1986) 481.
[17] G.H. Bogush, M.A. Tracy, C.F. Zukoski, J. Non-Cryst. Solids 104 (1988) 95.
[18] A.P. Philipse, A. Vrij, J. Colloid Interface Sci. 128 (1989) 121.
[19] J.-D. Lee, S.-M. Yang, HWAHAKKONGHAK 35 (1997) 782.
[20] J.-D. Lee, S.-M. Yang, J. Colloid Interface Sci. 205 (1998) 397.
[21] J.-D. Lee, S.-M. Yang, Korean J. Rheology 10 (1998) 24.
[22] J.-D. Lee, J.-H. So, S.-M. Yang, J. Rheology 43 (1999) 1117.
[23] M.-H. Oh, J.-H. So, J.-D. Lee, S.-M. Yang, Korean J. Chem. Eng. 16 (1999) 532.
[24] J.-H. So, S.-M. Yang, J.C. Hyun, Chem. Eng. Sci. 2001, in press.
[25] J.W. Bender, N.J. Wagner, J. Colloid Interface Sci. 172 (1995) 171.
[26] J.W. Bender, N.J. Wagner, J. Rheology 40 (1996) 899.
[27] G. Bossis, J.F. Brady, J. Chem. Phys. 91 (1989) 1866.
[28] J.F. Brady, J. Chem. Phys. 99 (1993) 567.
[29] J.F. Brady, J.F. Morris, J. Fluid Mech. 348 (1997) 103.
[30] D.R. Foss, J.F. Brady, J. Fluid Mech. 407 (2000) 167.